Technetium-99m Galactosyl-Neoglycoalbumin: Preparation and Preclinical Studies

David R. Vera, Robert C. Stadalnik, and Kenneth A. Krohn*

Division of Nuclear Medicine, University of California, Davis, Medical Center, Sacramento, California

Technetium-99m galactosyl-neoglycoalbumin ([Tc]NGA), a labeled analog ligand to the hepatocyte-specific receptor, hepatic binding protein (HBP), was prepared and tested for labeling yield, stability, biodistribution, toxicity, and dosimetry. The ligand was synthesized by the covalent coupling of a carbohydrate bifunctional reagent, 2-imino-2-ethyloxymethyl-1-thiogalactose, to human serum albumin. Testing in mice and rabbits revealed the product to be nontoxic and apyrogenic. Technetium labeling yields in excess of 95%, by the electrolytic method, did not alter the molecular weight profile of the neoglycoalbumin. The NGA-bound activity remained stable for at least 4 hr. Biodistribution studies in rabbits demonstrated the liver as the single focus of tracer uptake. Dosimetry was based on kinetic studies in three baboons. Absorbed doses to liver, small intestine, urinary bladder wall, and uterus were 0.089, 0.28, 0.56, and 0.88 rad/mCi, respectively. Total body, lens of the eye, red marrow, ovaries, and testes were less than 0.06 rad/mCi. High liver specificity imparted by receptor binding combined with high labeling yield, stability, acceptable dosimetry, and safety provide [Tc]NGA with the attributes required for routine clinical assessment of hepatocyte function.

J Nucl Med 26:1157–1167, 1985

We have proposed the use of hepatic binding protein (HBP) (*1*) as the target for functional imaging of the liver (*2*). This receptor, which resides only at the cell surface of hepatocytes, selectively binds galactose-terminated glycoproteins for transport to hepatic lysosomes (*3*).

Although we successfully used asialoceruloplasmin to deliver radioactivity to HBP (*4*), routine use in humans would be inevitably limited due to a variety of practical considerations. Native HBP ligands require enzymatic treatment. Moreover, clinical experience with the parent molecules, plasma glycoproteins, was sparse. We concluded that a more clinically acceptable radiopharmaceutical would be achieved by modification of a more appropriate protein. Thus, instead of removing terminal sialic acid groups to expose the HBP substrate, galactose, a synthetic analog was obtained by attaching the galactosyl unit to human serum albumin (HSA). The resulting compound is galactosyl-neoglycoalbumin (NGA).

We have reported (*5*) affinity-dependent and dose-dependent uptake of technetium-labeled NGA in animal models. These two properties satisfy the criterion of kinetic sensitivity (*6*) to receptor affinity and concentration, and thus indicate that in vivo measurements of these biochemical parameters may be obtained from [Tc]NGA uptake data.

In this paper we present data pertaining to the classical criteria for radiopharmaceutical quality: high labeling yield and stability, safety, high organ specificity, and acceptable dosimetry.

MATERIALS AND METHODS

Radiopharmaceutical preparation

Of the many methods available for the attachment of sugars to proteins, amidination using 2-imino-2-methoxyethyl-1-thioglycosides (*7*) was chosen. This reagent is specific for primary amino groups, and the coupling can be carried out at a mild pH (*7*). Also, the pK_a's of ϵ

Received Dec. 10, 1984; revision accepted Jun. 20, 1985.

For reprints contact: Robert C. Stadalnik, M.D., Division of Nuclear Medicine, University of California, Davis, Med. Ctr., 2315 Stockton Blvd., Room G206, Sacramento, CA 95817.

* Present address: Division of Nuclear Medicine, University of Washington Hospital, Seattle, WA.

amines and imino hydrogens are similar (*8*). This maintains the charge distribution within the macromolecule and thus minimizes alteration in tertiary structure of the modified protein (*9*). Significant alteration in the conformation of the protein backbone could result in reticuloendothelial uptake. The amidine bond (*9*) and thioesters (*10*) are stable under acidic conditions which are required for technetium labeling through the electrolytic method. Thioesters are also resistant to plasma and membrane glycosidases (*11*). Thus, the resulting ligand should be stable in vivo.

We selected HSA as the protein backbone for a variety of reasons. First, and most significant is its availability at a low cost in a sterile apyrogenic form. Second, the product is also heat-treated against the possibility of transmitting the hepatitis virus. Third, its high molecular weight minimizes glomerular filtration and interstitial diffusion from the vasculature. Fourth, a variety of techniques exist by which this protein can be labeled with technetium-99m (^{99m}Tc). Thus, although we initiated the development of [Tc]NGA with the electrolytic method, we anticipate the use of an "instant" kit based on chemical reduction. Lastly, labeled HSA was designed for imaging vascular structures. As a result, [Tc]HSA is stable in vivo, and remains in the vasculature for an extended period of time. Thus, during the course of a [Tc]NGA imaging study one could expect the labeled HSA to serve as a neutral carrier for the receptor substrate, galactose.

Beginning with galactose **1** and bromine in acetic anhydride 2,3,4,6-tetra-*O*-acetyl-α-D-galactopyranosyl bromide **3** was produced through the method described by Bárczai-Martos (*12*). After crystallization (−20°C, 8 hr) and filtration compound **3** was reacted with thiourea in acetone (*13*) to yield 2-*S*-(2,3,4,6-tetra-*O*-acetyl-β-D-galactopyranosyl)-2-thiopseudourea hydrobromide **4**. Following the procedure outlined by Lee (*7*), cyanomethyl-2,3,4,6-tetra-*O*-acetyl-β-D-galactopyranoside **5** was synthesized. This product was twice recrystallized and then decolorized to remove any hydrophobic chromophore which could bind to albumin and possibly produce a toxicologic effect or a decrease in the technetium labeling yield. Compound **5**, the most stable in the reaction sequence, was chosen as the point of storage (−20°C, for at least 5 yr).

Preparation of sterile apyrogenic neoglycoalbumin required aseptic technique during the last four steps. This included: (a) formation of the coupling reagent (*7*) 2-imino-2-methoxyethyl-1-thio-β-D-galactopyranoside **6** (IME-thiogalactose), (b) rotary evaporation of the product and recovery into aqueous buffer, (c) coupling of IME-thiogalactose to HSA, and (d) diafiltration of the resulting neoglycoalbumin to remove unreacted coupling reagent.

Aqueous solutions were prepared using USP irrigation solutions*. The diafiltration system†, metal, teflon parts, and plasticware were thoroughly washed in detergent‡ solution of glass-distilled water, rinsed with irrigation water, air-dried, and then gas-sterilized. Glassware was acid-cleaned prior to the above procedure. The diafiltration system without the ultrafiltration membrane was assembled in a chromatographic cold box. A gas-sterilized 0.2 μ filter housed in a stainless steel holder was placed between the ultrafiltration system and the pressure source, a regulated (30 psi) nitrogen gas cylinder. The ultrafiltration membrane§ was immersed for 30 min in a beaker containing a stirred solution of Clorox (0.01%)¶.

After measurement of IME-thiogalactose (*14*), the methanol was removed by way of rotary evaporation under reduced pressure. The resulting solid was then resolubilized by the addition of freshly prepared Clark's borate buffer (pH 8.6, 0.2*M*). Carbohydrate density of the neoglycoalbumin, the number of galactose units per albumin molecule, was controlled by the molar ratio of the starting reagents (*6*), IME-thiogalactose and HSA. Thus, based on the IME-thiogalactose yield and the desired carbohydrate density, an amount of HSA** was added to the reaction mixture, which was then allowed to incubate at room temperature for 3 hr. During this time, the membrane and ultrafiltration were sequentially treated with the following solutions: (a) 1*M* phosphoric acid, 25°C, 30 min, (b) 0.05N sodium hydroxide, 80°C, 60 min, and (c) four changes of 80°C water, 15 min each. After installation of the membrane, the neoglycoalbumin solution was transferred via a 0.2 μ filter to the ultrafiltration cell, and immediately dialyzed against five exchange volumes of isotonic saline; after which the solution was concentrated to 12% (w/v), then transferred to a sterile multidose vial by way of a 0.45 μ filter. Samples were retained for analysis of carbohydrate density (*15*), albumin concentration ($a_m = 4 \times 10^4 M^{-1}cm^{-1}$, 280 nm), sterility (USP 71) and apyrogenicity (USP 85 and 151). The ultrafiltration membrane was aseptically removed, placed working-side down on a blood agar plate, and tested for sterility.

Labeling and quality control

The electrolytic method developed by Benjamin (*16*) was used to label galactosyl-neoglycoalbumin with ^{99m}Tc. The protocol described by Dworkin (*17*) for the closed-system preparation of [Tc]HSA was utilized with the following modifications. Electrolysis cells were constructed using 10 ml multidose vials. Acid solution was not added to the electrolysis cells prior to sterilization. The reactants were added in the following sequence: (a) 3 ml saline, pH 1.2, (b) NGA, 25 mg, and (c) [^{99m}Tc]pertechnetate‡‡ in 2 ml isotonic saline containing the desired amount of radioactivity. Prior to application of current (50 mA), the cell was purged with nitrogen for 10 min. Neutralization of the product

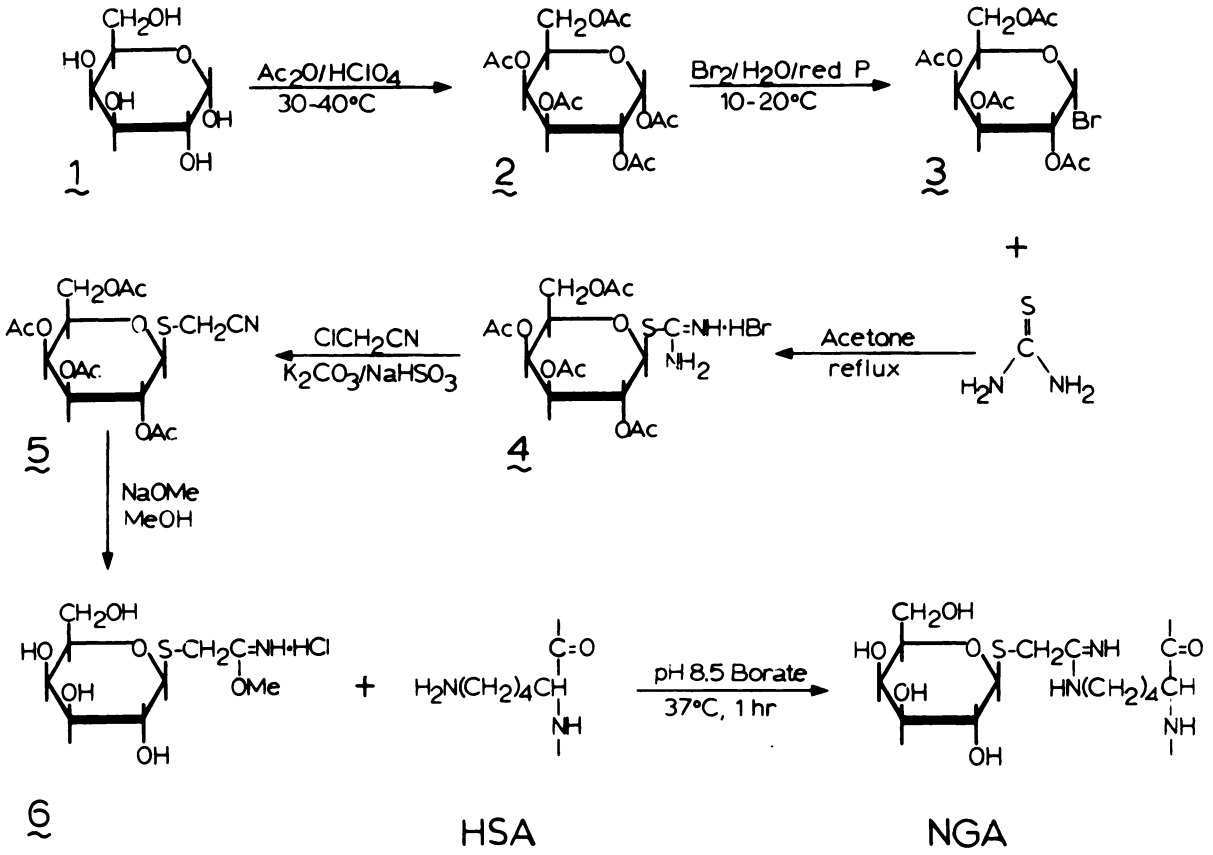

FIGURE 1
Reaction scheme for synthesis of galactosyl-neoglycoalbumin (NGA). Reaction sequence from 5 to NGA, and separation of 6 from NGA were carried out under sterile apyrogenic conditions

was accomplished with 0.6 ml of bicarbonate buffer (*17*).

Two forms of radiochemical quality control were used. Electrophoresis (250 V, 20 min) was carried out on polyacetate strips†† (2 × 25 cm) in barbital buffer (pH 8.6, 25°C)††. Strips were scanned with a collimated sodium iodide detector (*18*). High performance liquid chromatography (HPLC) was performed immediately, and 10 hr after labeling using a TSK-3000SW column (7.5 × 300 mm)§§ eluted isocratically (1.0 ml/min) with isotonic saline. The eluate was monitored with an ultraviolet detector at 254 nm and a sodium iodide scintillation detector.

Testing for acute and subacute toxicity

Two acute toxicity studies were performed using mice. The first study utilized three groups of female BALB/c mice (~25 g). Twelve mice were injected with 0.4 ml of 25% (w/v) HSA**, and another 12 were injected with 0.4 ml isotonic saline. Seven mice were injected with 0.4 ml of an NGA preparation averaging 21 galactose groups per HSA molecule (NGA-21). The concentration of the NGA dose was adjusted such that each mouse received 10 mg NGA-21 per kg of body weight. This dose represented 200 times the scaled human dose (0.05 mg/kg). The second acute toxicity study used two groups of male Swiss/Webster mice (~25 g). Six mice were administered 0.3 ml saline. An additional 24 mice were injected with 7.5 mg of NGA-44 in a volume of 0.3 ml. This dose exceeded the scaled human dose by 5,000-fold. All animals were observed over the 24-hr period after injection.

Testing for acute toxicity was also carried out in ten rabbits (New Zealand White, five female, five male, ~3 kg), at 700 times the scaled human dose. A control group of five animals (two female, three male) received saline injections of equal volume (0.2 ml). Prior to injection, each animal was sedated with 0.5 ml thorazine subcutaneously. Blood samples (12 ml) were obtained from the central auricular artery for complete blood count (CBC) and serum analysis (SMA). The urinary bladder was tapped percutaneously for a urinalysis sample. Saline or NGA was then injected in the posterior marginal ear vein. Each rabbit was observed for any evidence of malaise, anorexia, depression (poor posture, droopy ears), lethargy or dyspnea. Food and water intake, and weight were also monitored. Twenty-four hours after injection, each rabbit was sedated for CBC and SMA collection, anesthetized (200 mg ketamine i.m.) and exsanguinated by cardiac puncture.

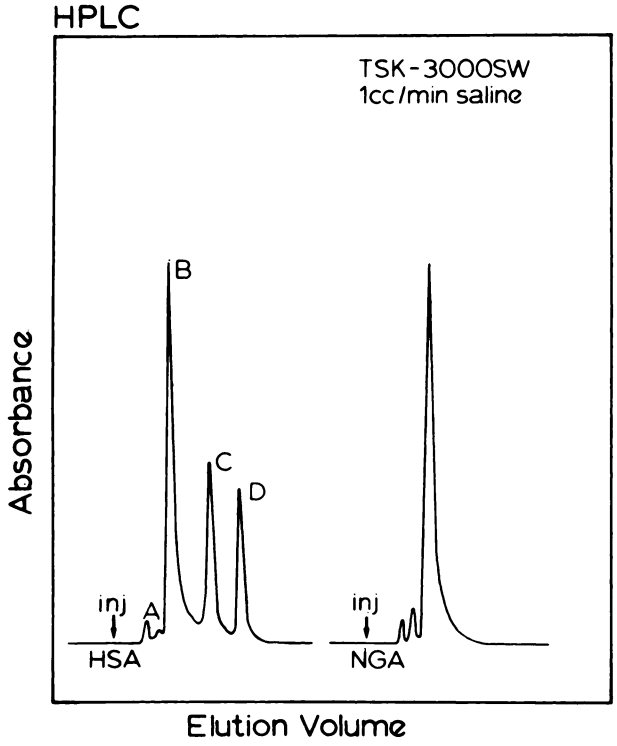

FIGURE 2
HPLC of HSA and NGA. Coupling of galactose to HSA did not alter the molecular weight distribution of the protein. The small peaks (A) are IgG, trimeric and dimeric albumin. Peak B is monomeric albumin, C and D are stabilizers, caprolic acid and acetyltryptophan

Urinary bladder was sampled, and the following tissues were necropsied and fixed in 10% formalin solution: enteric lymph node and bone marrow smears, liver, heart, spleen, gallbladder, kidneys, lungs, colon, ileum, stomach, brain, eyes, urinary bladder, lymph node, gonad, muscle, bone, and injection site (pinna). Student's t-test was used to compare control and test groups for significant alterations in CBC, SMA, and urine values.

Testing for subacute toxicity was performed in rabbits in the following manner. On 14 consecutive days at 24 hr intervals, three groups of five animals received either five or 50 times the expected administered dose per kg or isotonic saline. Prior to injection, blood and urine samples were obtained as previously described. Samples were also obtained on the seventh and fourteenth day of the study at which each animal was killed and the necropsies performed as described above. All injections were in the marginal ear vein. Food and water intake were monitored daily. Statistical analyses were performed using least squares linear regression to determine if there was correlation between dose levels and blood or urine parameters.

Biodistribution studies

New Zealand White rabbits (68–73 days, 1.9–2.2 kg) were used to measure the tissue distribution of [Tc]NGA-21 (0.05 mg/kg) and [^{125}I]HSA[¶¶] at 3 and 60 min. One female and one male were used at each point. The animals were fasted during the 24-hr period prior to the study. Animals under anesthesia (xylazine, 5 mg/kg i.m.; ketamine, 50 mg/kg i.m.) were injected in the marginal ear vein. The [^{125}I]HSA (column-purified; 2.5 × 75 cm, G-200) dose (~0.1 μCi) was administered immediately after the [Tc]NGA. At the indicated time the animals were killed (T-61***, 0.3 ml/kg) and blood was sampled through cardiac puncture. Vessels leading to the liver were clamped; the organ was then removed, weighed, and homogenized. With the exception of muscle and bone, organs were removed whole and dispensed into plastic sample vials. Samples and dose standards were assayed for ^{99m}Tc activity using a 100–200 keV window and ^{125}I activity (10 days after the study) using a 20–40 keV window. Calculation of total blood volume was based on ^{125}I activity of the blood samples. Muscle and bone were assumed to constitute 40 and 10% of total body weight (*19*).

Three baboons (*Papio cynocephalus*) were studied twice (1 wk apart) with [Tc]NGA-21. Each animal received 0.05 mg/kg. Computer acquisition[†††] of the gamma camera data was initiated during administration of the radiopharmaceutical. Digital images (64 × 64 pixels) were acquired in byte mode at a rate of eight frames per min. At 3 min postinjection, ~1 ml of blood was sampled, and placed in a preweighed plastic tube. Computer acquisition was halted 1 hr after injection.

The blood sample and a dose standard were assayed for radioactivity (100–200 keV window). Time-activity curves for the blood and liver were generated by selecting regions-of-interest around the heart and lungs, and the left lobe of the liver. Based on the following assumptions, liver and blood time-activity curves were scaled to percentage of injected dose: (a) the total blood volume of each baboon was 7% of body weight (*20*), (b) blood volume within each liver was ~15% of total blood volume, and (c) at the time of the blood sample (3 min PI), all [Tc]NGA not residing within the blood was bound to hepatocytes. The first is a standard and reasonable assumption when calculating percent of injected dose within the blood of a healthy subject. Error contributed by the second assumption is small in the presence of active hepatocyte clearance. For example, if at 3 min postinjection 20% of the ^{99m}Tc activity is within the blood, 15% of this value will reside within the liver. Three percent of the [Tc]NGA dose is small compared to the 80% which is bound to the hepatocyte receptor. The third assumption was validated by the rabbit biodistribution studies.

Dosimetry calculations

Calculation of the radiation absorbed doses to a human resulting from an i.v. administration of

[^{99m}Tc]NGA were based upon rabbit biodistribution and baboon biokinetic data, and the MIRD tables (*21*). A three compartment model, similar to the parent-daughter decay scheme of a radioisotope generator system, was used to quantitate the time-activity data obtained from the baboon studies. This model assumes irreversible binding of [Tc]NGA by the receptor. The magnitude of the association constant for [Tc]NGA binding, $10^9\ M^{-1}$, (*6*) permits this assumption. The solution to this model is attributed to Bateman (*22*). Correcting for radioactive decay by multiplication of the Bateman Equations by $e^{-\lambda t}$ gives

$$A_{BL}(t) = A_{BL}(0)\exp[-(k_1 + \lambda)t] \quad (1)$$

$$A_{LI}(t) = \frac{A_{BL}(0)k_1}{k_1 - k_2} \times [\exp[-(k_1 + \lambda)t] - \exp[-(k_2 + \lambda)t]] \quad (2)$$

$$A_P(t) = A_{BL}(0)\left[\exp[-\lambda t] - \frac{k_2\exp[-(k_1 + \lambda)t] - k_1\exp[-(k_2 + \lambda)t]}{k_2 - k_1}\right]. \quad (3)$$

Where at time t, $A_{BL}(t)$, $A_{LI}(t)$, and $A_P(t)$ represent ^{99m}Tc activity in blood, liver, and deposition sites of labeled metabolic product. Integration from time zero to infinity yields the cumulated activity within each organ: $\tilde{A}_{BL}(\infty)$, $\tilde{A}_{LI}(\infty)$, and $\tilde{A}_P(\infty)$.

$$\tilde{A}_{BL}(\infty) = \frac{A_{BL}(0)}{k_1 + \lambda} \quad (4)$$

$$\tilde{A}_{LI}(\infty) = \frac{A_{BL}(0)k_1}{k_2 - k_1}\left[\frac{1}{k_1 + \lambda} - \frac{1}{k_2 + \lambda}\right] \quad (5)$$

$$\tilde{A}_P(\infty) = A_{BL}(0)\left[\frac{1}{\lambda} - \frac{\frac{k_2}{k_1 + \lambda} - \frac{k_1}{k_2 + \lambda}}{k_2 - k_1}\right] \quad (6)$$

Parameters k_1 and k_2 were obtained from liver time-activity data (decay-corrected) of each baboon study by standard curve-fitting techniques (*23*). The mean of each parameter and λ for ^{99m}Tc ($0.12\ hr^{-1}$) were then substituted into Eqs. (4)-(6) to calculate the mean cumulated activity within the blood and liver [$\tilde{A}_{BL}(\infty)$, $\tilde{A}_{LI}(\infty)$], and the mean cumulated activity associated with metabolic product [$\tilde{A}_P(\infty)$]. Based on the 60 min rabbit biodistribution data, the small intestine and urinary bladder were selected as the deposition sites of the labeled metabolic product. The cumulated activity within each organ ($\tilde{A}_{SI}(\infty)$, $\tilde{A}_{BLADC}(\infty)$) was calculated based on Eqs. (7) and (8).

$$\tilde{A}_{SI}(\infty) = f_1\tilde{A}_P(\infty) \quad (7)$$

$$\tilde{A}_{BLADC}(\infty) = f_1\tilde{A}_P(\infty) \quad (8)$$

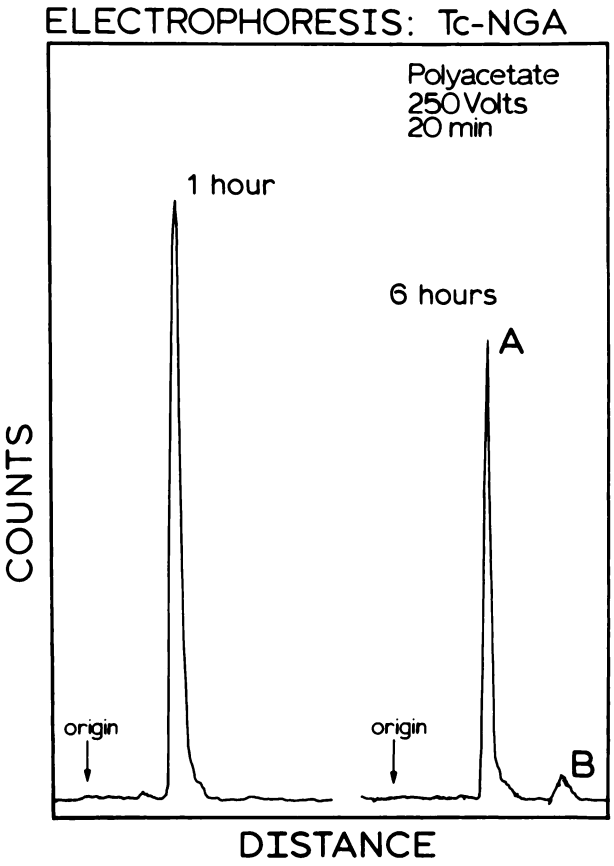

FIGURE 3
Quality control of [Tc]NGA. Electrophoresis on polyacetate strips (250V, 20 min, 25°C) can separate reduced unbound technetium (origin), [Tc]NGA (A), and unbound pertechnetate (B) which appeared 4–6 hr after labeling

Fractions, f_1 and f_2, represent the relative distribution of activity between the two organs. Activity within the blood was considered equivalent to the total-body source; thus, $\tilde{A}_{TB}(\infty)$ was set equal to $\tilde{A}_{BL}(\infty)$. Using S-Factors, $S(r_k \leftarrow r_h)$, for ^{99m}Tc (*21*), and cumulated activities, $\tilde{A}_h(\infty)$, from the four source organs, the absorbed radiation doses, $\bar{D}(r_k)$, to liver, small intestine, urinary bladder wall, total body, red marrow, ovaries, uterus, and testes were calculated using

$$\bar{D}(r_k) = \sum_h \tilde{A}_h S(r_k \leftarrow r_h) \times 1{,}000 \quad \text{(rad/mCi)}.$$

RESULTS

Radiopharmaceutical preparation

Starting with 100 g of galactose **1**, 80 g of compound **5** could be obtained after repeated recrystalization. The average number of galactose groups per albumin molecule (Gal/HSA) could be preselected to within 20% by

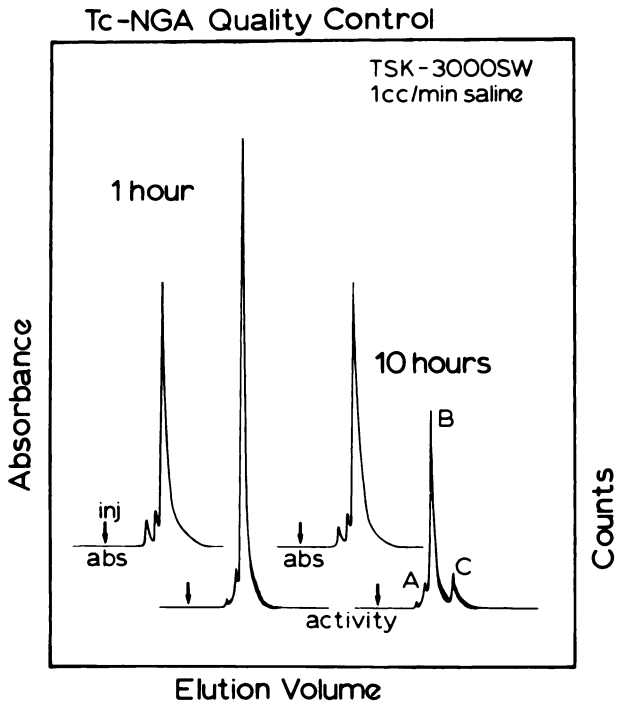

FIGURE 4
HPLC quality control of [Tc]NGA. Radioactivity and absorbance (254 nm) profiles at 1 hr revealed high labeling yields and minimum alteration of molecular weight distribution (see Fig. 2). Ten hours after labeling, unbound pertechentate appeared (Peak C). Peak B represents monomeric [Tc]NGA. Polymeric [Tc]NGA eluted at A

using the following linear relationship: Gal/HSA = 4.5 + 0.12 × IME/HSA. Where, IME/HSA represents the molar ratio of compound **6** to HSA. Seven lots of NGA were prepared using the diafiltration system, the solution volumes ranged from 80 to 180 ml. Diafiltration in the cold (5°C) of 150 ml of a NGA/IME-thiogalactose solution with five exchange volumes of normal saline required ~20 hr. An additional 5 hr was required to concentrate the solution to a final concentration of 12%. Routine protein recovery from this process was 90%.

All NGA preparations and ultrafiltration membranes passed sterility (USP 71) and pyrogen (USP 85, USP 151) testing. One NGA solution (13%, 37 gal/HSA) passed USP 71 and USP 151 testing after 3 yr of refrigerated storage. Gel filtration/HPLC revealed minor differences between the absorbance profiles of the starting reagent, HSA, and the product, NGA. The difference was a slight increase in dimeric NGA (peak A, Fig. 2), and eluation volume of the product. Preparations of high carbohydrate density, for example NGA-37, exhibited a 5% increase relative to HSA monomer (peak B, Fig. 2).

Technetium labeling

Labeling of NGA with technetium by way of the electrolytic method produced a technetium-NGA label without formation of aggregates or protein polymers. The labeling yield of the first 100 products as measured by HPLC ranged from 92–99%. The majority of labeling yields were in excess of 96%, which was selected as the minimum value for an acceptable product. The product was stable for at least 4 hr. The radiochromatographic scans of Fig. 3 are the result of polyacetate electrophoresis of the [Tc]NGA-21 used for the rabbit biodistribution study, and are representative of electrophoresis quality control at 1 and 6 hr after labeling. After 4 to 6 hr, a peak representing unbound pertechnetate would appear 6.2 cm from the origin.

Technetium-NGA quality control using TSK-3000 HPLC showed a similar pattern with regard to label

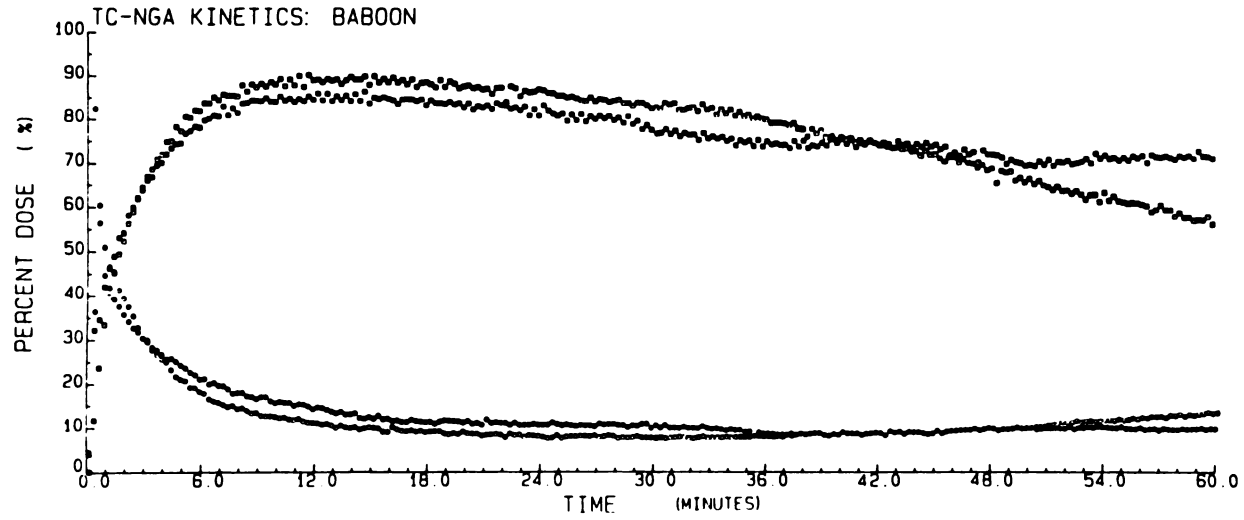

FIGURE 5
[Tc]NGA kinetics in two baboons using NGA-21 at dose of 0.05 mg per kg of body weight. Two studies representing highest (open symbols, baboon #2) and lowest (closed symbols, baboon #3) metabolic activity are illustrated (□) Liver; (■) Liver; (○) Blood; (●) Blood

stability (Fig. 4). Unbound pertechnetate would appear (peak C, Fig. 4) 6 to 8 hr after labeling. Absorbance and radioactivity profiles indicated that the technetium preferentially bound to the NGA monomer; ~90% of the protein existed as NGA monomer, but more than 95% of the activity eluted with the monomeric peak.

Biological safety

No abnormal behavior was observed during the 24-hr period after acute injection of NGA into mice or rabbits. Statistical analysis of blood and urine parameters resulting from the acute (500X) injections into rabbits found no significant ($p < 0.1$) differences between control (saline injection) and test (NGA injection) animals. Prior to injection, however, statistically significant differences between control and test groups existed for three parameters.

1. The plasma protein level of the control group (6.85 ± 0.34 g/dl) was higher than the test group (6.10 ± 0.29 g/dl) ($p < 0.005$).
2. The mean corpuscular volume of the control group (70.0 ± 2.0 ml) was higher than the test group (66.2 ± 3.5 ml) ($p < 0.05$).
3. The specific gravity of the urine for the control group (1.033 ± 0.006) was higher than that of the test animals (1.025 ± 0.007) ($p < 0.025$).

Subacute toxicity data of Days 1 and 7 revealed no statistically significant ($p < 0.1$) correlations between NGA dose and any blood or urine parameter. On the fourteenth day, statistically significant correlations were found between heterophils and dose level (heterophils = 66.23 cells + dose × 0.59 cells/ml; $r = -0.66$, $df = 10$, $p < 0.05$), lymphocytes and dose level (lymphocytes = 30.0 cells + dose × 0.59 cell/ml; $r = 0.60$, $df = 10$, $p < 0.02$). Histologic examination of bone marrow aspirates and lymph node smears revealed no evidence of toxicity of pathologic significance. Complete details of these studies have been submitted with a Notice of Claimed Investigational Exemption for a New Drug.[‡‡‡]

Biodistribution and dosimetry

Absolute and scaled (per gram of tissue) uptakes for ^{125}I and ^{99m}Tc activities are listed in Table 1. At 3 min postinjection, the ^{99m}Tc activity in the liver and blood summed to within 10% of the injected dose. The significant features of this data in regard to dosimetry are the following.

1. At 3 min after [Tc]NGA injection only the liver contained more ^{99m}Tc than ^{125}I activity.
2. At 60 min only five organs, kidneys, urinary bladder and urine, small intestine, gallbladder, and thyroid, contained more ^{99m}Tc than ^{125}I. The latter two organs, gallbladder and thyroid, held less than 1% of the ^{99m}Tc dose.
3. The femur (representing blood-forming tissue), eyes, and gonads contained less than 1% of the ^{99m}Tc dose at the 3 and 60-min time points.
4. At 60 min ^{99m}Tc in the GI tract (small intestine, gallbladder, and large intestine) was roughly equal to the activity within the kidney, urinary bladder wall, and urine.

Liver uptake in normal baboons peaked within 12 to 15 min after injection. At this time the activity within the liver represented 80 to 90% of the injected dose. The rate of hepatic metabolism for each baboon varied between each study. Figure 5 displays liver and heart/lung time-activity curves from baboons which exhibited the highest and lowest metabolic activity. Values for kinetic parameters, representing the rates of hepatic extraction, k_1, and metabolism, k_2, and absorbed doses resulting from similar kinetics in humans are listed in Table 2. Mean values for k_1 (12.8 ± 3.1 hr^{-1}) and k_2 (0.442 ± 0.313 hr^{-1}) were used to calculate a mean absorbed radiation dose to a human with normal hepatic function (Table 2). The calculations assumed that the metabolic products of [Tc]NGA were equally distributed between the urinary and GI tracts (f_1 and f_2 equal 0.5). The mean absorbed radiation doses in units of rad/mCi were: liver, 0.089; small intestine 0.28; urinary bladder wall, 0.56; total body, 0.019; red marrow 0.025; ovaries, 0.064; uterus, 0.088; and testes, 0.019. Because the biodistribution data at 3 and 60 min demonstrated a lack of active [Tc]NGA uptake by the eyes, the mean absorbed radiation dose for the lens of the eye was considered to be equal to the total-body dose.

DISCUSSION

Technetium labeling

Since [Tc]NGA was intended as a hepatocyte-specific radiopharmaceutical, the labeling procedure could not yield colloidal products which would localize to reticuloendothelial cells. Size-exclusion chromatography was a sensitive measure of polymer formation. However, because macroaggregates of NGA and colloidal material could not pass through the column and thus be detected, we augmented our quality control with electrophoresis. These procedures indicated that although the electrolytic method could routinely produce a labeled product free of [Tc]NGA polymers, colloidal contaminants would result when the first elution of a new technetium generator was used. Also, maximum labeling yields were obtained when the vial containing the labeling reactants were purged with nitrogen for at least 10 min.

Biological safety

We have presented the criterion of "kinetic sensitivity" in regard to the performance of functional imaging

TABLE 1
Rabbit Biodistribution of [Tc]NGA-21 and [^{125}I]HSA

Organ	Time after injection (min) 3				60			
	^{99m}Tc*		^{125}I		^{99m}Tc		^{125}I	
	% ID	% ID/g	% ID	% ID/g	% ID	% ID/g	% ID	% ID/g
Liver	73.	0.68	26.	0.29	4.1	0.051	25.	0.31
	78.	1.1	24.	0.33	18.	0.25	23.	0.32
Blood	18.	0.11	100.	0.61	4.7	0.029	100.	0.62
	19.	0.14	100.	0.72	4.0	0.026	100.	0.65
Urine	0.050	—	0.12	—	16.	—	0.11	—
	0.37	—	0.15	—	18.	—	0.18	—
Kidneys	3.3	0.15	3.2	0.15	7.6	0.55	2.1	0.15
	3.4	0.21	2.3	0.14	5.7	0.40	2.5	0.18
Urinary bladder	0.040	0.010	0.083	0.021	0.027	0.032	0.0064	0.0076
	0.018	0.015	0.028	0.023	0.16	0.19	0.062	0.0070
Small intestine†	0.74	—	2.4	—	33.	—	0.14	—
	0.70	—	1.6	—	30.	—	2.2	—
Gallbladder†	0.028	—	0.042	—	0.031	—	0.0022	—
	0.074	—	0.045	—	1.3	—	0.0027	—
Bone, femur	0.44	0.0016	3.8	0.011	0.58	0.0018	4.1	0.013
	0.61	0.0022	5.0	0.015	0.91	0.0028	5.4	0.017
Bone, rib	1.7	0.0075	7.6	0.034	3.2	0.016	3.2	0.016
	5.5	0.026	13.	0.060	4.4	0.023	11.	0.014
Muscle, flank	7.7	0.0085	24.	0.027	1.5	0.0018	14.	0.017
	7.1	0.0081	19.	0.022	5.4	0.0071	10.	0.014
Heart	0.68	0.058	2.9	0.25	0.093	0.014	1.6	0.25
	0.80	0.97	3.2	0.29	0.15	0.017	2.3	0.26

Lung	1.4	0.068	6.0	0.30	0.17	0.014	5.3	0.42
	2.2	0.12	6.6	0.36	0.47	0.021	9.1	0.40
Spleen	0.081	0.081	0.16		0.032	0.070	0.68	0.19
	0.086	0.14	0.067	0.11	0.026	0.053	0.062	0.13
Brain	0.015	0.023	0.034	0.0052	0.036	0.0040	0.12	0.015
	0.032	0.0038	0.13	0.015	0.0083	0.0012	0.085	0.012
Stomach†	0.31	—	0.78	—	0.41	—	0.25	—
	0.13	—	0.80	—	0.32	—	0.97	—
Large intestine†	0.60	—	1.3	—	0.67	—	0.32	—
	0.75	—	1.4	—	1.4	—	2.2	—
Thyroid	0.0053	0.020	0.0067	0.025	0.11	0.55	0.0047	0.025
	0.072	0.026	0.0092	0.033	0.073	0.23	0.0093	0.028
Thymus	0.034	0.0084	0.094	0.023	0.038	0.0070	0.038	0.0070
	0.037	0.013	0.096	0.033	0.047	0.0086	0.024	0.0054
Eyes	0.014	0.0027	0.075	0.015	0.042	0.0080	0.016	0.0032
	0.023	0.0044	0.044	0.0084	0.017	0.0062	0.058	0.014
Testes	0.059	0.011	0.18	0.032	0.041	0.011	0.038	0.010
	NA‡	NA	NA	NA	NA	NA	NA	NA
Ovaries	NA	NA	NA	NA	NA	NA	NA	NA
	0.013	0.027	0.037	0.080	0.014	0.10	0.14	0.064
Injection site	0.046	—	0.15	—	0.17	—	0.13	—
	0.078	—	0.17	—	0.067	—	0.16	—
I.V. Line	0.32	—	0.15	—	0.96	—	0.80	—
	0.27	—	0.22	—	0.17	—	0.85	—

* Dose: 0.05 mg/kg, 7.4×10^{-10} mol/kg.
† Including contents.
‡ Not available.

TABLE 2
Human Dosimetry

Baboon	Rate constant* (hr^{-1}) k_1	k_2	Absorbed radiation dose† (rad/mCi) Liver	Small intestine	Urinary bladder wall	Red marrow	Ovaries	Uterus	Testes
1	17.	0.30	0.12	0.26	0.51	0.024	0.058	0.081	0.018
1	12.	0.36	0.10	0.27	0.53	0.025	0.061	0.086	0.018
2	9.0	0.48	0.083	0.28	0.56	0.025	0.064	0.090	0.019
2	10.	0.96	0.050	0.31	0.62	0.027	0.071	0.10	0.020
3	14.	0.54	0.077	0.29	0.58	0.026	0.066	0.10	0.019
3	15.	0.012	0.36	0.046	0.068	0.015	0.011	0.014	0.0093
Mean‡	12.8	0.442	0.089	0.28	0.56	0.025	0.064	0.088	0.019
± s.d.	3.1	0.313	—	—	—	—	—	—	—

* $\lambda = 0.115\ hr^{-1}$.
† values based on k_1 and k_2 from each study, or means of k_1 and k_2; total body, and lens of eye equaled 0.019 rad/mCi.
‡ k_1 and k_2 only.

agents (*6*). This concept states that if a physiochemical parameter is to be estimated from in vivo time-activity data, the parameter must control the shape of the time-activity curve. A parameter controls the uptake of tracer if a change in the parameter's value alters the kinetic data. Our in vivo studies (*5*) of [Tc]NGA kinetics demonstrated that the shape of liver time-activity curves were dependent upon the molar dose of [Tc]NGA. Thus, the [Tc]NGA time-activity data was sensitive to the concentration of receptor when an appropriate amount of ligand was injected. In addition, kinetic simulations (*24*) indicated that in vivo estimates of receptor concentration will require that at least 10% of the receptors be occupied by the radioligand. Our toxicity studies demonstrated a high margin of safety; the 10% ligand-to-receptor ratio, which translates to 7.4×10^{-10} mole NGA per body weight (0.05 mg NGA/kg), could be exceeded by a factor of 700 in a single dose without adverse effects in rabbits or mice.

Biodistribution and dosimetry

Biodistribution studies in rabbits and baboons demonstrated that the liver was the only tissue which selectively accumulated [Tc]NGA. Low uptake values for tissues other than liver correlated with rabbit (*5*) and baboon imaging in which only the liver was visualized at 20 min postinjection. Besides producing excellent images, uptake resulting from accumulation by a single organ simplifies the analysis of [Tc]NGA kinetics. First, the number of compartments within the kinetic model is minimized. Second, at early times during the uptake phase of [Tc]NGA, time-activity curves representing blood and liver will sum to the amount injected. This property will allow conservation of mass (mole of NGA) during simulation of early time points of the kinetic model. As a result, it will be possible to approximate the amount of [Tc]NGA in the liver at a given time by sampling activity within the blood at that time. Use of standard kinetic techniques for determination of tracer distribution volume (*25*) would then permit scaling of liver time-activity curves to percentage of the [Tc]NGA dose.

As indicated by the liver time-activity curves (Fig. 5), there was a slow but variable degree of metabolism. The low rate of exit from the liver will provide ample time to acquire dynamic images. Hepatic metabolism of [Tc]NGA significantly diminishes the absorbed dose to the liver when compared to [Tc]sulfur colloid (0.34 rad/mCi) (*26*). Our calculations did not include urination, which occurring at 4 hr intervals would substantially diminish the absorbed dose to the gonads and bladder wall. The gallbladder of the baboon with the highest metabolic rate constant, k_2, was faintly visualized 65 min after injection. We do not anticipate, however, that gallbladder or GI activity will impair static liver images which will be acquired between 20 to 40 min postinjection.

Significance

Technetium-galactosyl-neoglycoalbumin is the first technetium-based radiopharmaceutical which exhibits in vivo receptor-binding properties (*5*). The availability of ^{99m}Tc and its compatibility with standard imaging instrumentation will permit the use of this receptor-binding radiotracer on a routine basis. Moreover, by utilizing the receptor properties of NGA-HBP binding, it will be possible to optimize the extraction of physiologic information from time-activity data (*24*) by chemical manipulation of the synthetic ligand (*6*). Thus, [Tc]NGA offers an opportunity to combine chemical and engineering techniques to the design of an optimized functional imaging agent.

ACKNOWLEDGMENTS

This research was supported by grants from the American Cancer Society (#RD-61 and #PDT-180) and the New

England Nuclear Corporation. The authors are indebted to Drs. Bernard Feldman and Boris Reubner for review of the tissue samples from the toxicity studies, and Dr. Horace Hines for the statistical analysis of the blood and urine data. The authors also thank Dr. Nathaniel M. Matolo for providing the baboons, and Dusan Hutak and Scott Steffens for their excellent technical assistance.

FOOTNOTES

* Travenol, Deerfield, IL.
† Amicon, 202; Danvers, MA.
‡ Vestal Laboratories, 1-Stroke Ves-Phene, St. Louis, MO.
§ Amicon, YM-30; Danvers, MA.
¶ The Clorox Corporation, Oakland, CA.
** Cutter Laboratories, Plasbumin 25, Berkeley, CA.
††Gelman-Sciences, Ann Arbor, MI.
‡‡ Squibb Diagnostics, Minitec, New Brunswick, NJ.
§§ Beckman Instruments, Irvine, CA.
¶¶ Mallinckrodt, St. Louis, MO.
*** Taylor Pharmacal, Decatur, IL.
††† ADAC Laboratories, DPS-2200; San Jose, CA.
‡‡‡ IND 26,065, Food and Drug Administration, Rockville, MD.

REFERENCES

1. Stockert RJ, Morell AG: Hepatic binding protein: The galactose-specific receptor of mammalian hepatocytes. *Hepatology* 3:750-757, 1983
2. Krohn KA, Vera DR, Stadalnik RC: A complementary radiopharmaceutical and mathematical model for quantitating hepatic-binding protein receptors. In *Receptor-Binding Radiotracers*, Vol. II, Eckelman WC, ed. Boca Raton, Florida, CRC Press, 1982, pp 41-59
3. Ashwell G, Steer CJ: Hepatic recognition and catabolism of serum glycoproteins. *JAMA* 246:2358-2364, 1981
4. Vera DR, Krohn KA, Stadalnik RC: Radioligands that bind to cell-specific receptors: Hepatic binding protein ligands for hepatic scintigraphy. *Proceedings of the Second International Symposium on Radiopharmaceuticals II*. New York, Society of Nuclear Medicine, 1979, pp 565-575
5. Vera DR, Krohn KA, Stadalnik RC, et al: Tc-99m-galactosyl-neoglycoalbumin: In vivo characterization of receptor-mediated binding to hepatocytes. *Radiology* 151:191-196, 1984
6. Vera DR, Krohn KA, Stadalnik RC, et al: Tc-99m-galactosyl-neoglycoalbumin: In vitro characterization of receptor-mediated binding. *J Nucl Med* 25:779-787, 1984
7. Lee YC, Stowell CP, Krantz MJ: 2-Imino-2-methoxyethyl-1-thioglycosides: New reagents for attaching sugars to proteins. *Biochem* 15:3956-3963, 1976
8. Roger R, Neilson D: The chemistry of imidates. *Chem Rev* 61:179-211, 1961
9. Hunter MJ, Ludwig ML: Amidination. *Meth Enzymol* 25:585-596, 1972
10. Horton D, Hutson DH: Developments in the chemistry of thiosugars. *Adv Carbohydr Chem* 18:123-199, 1963
11. Monod J, Cohen-Bazire G, Cohn M: Sur la biosynthese de la β-galactosidase (lactase) chez *Escherichia coli*. La specificite de l'induction. *Biochim Biophys Acta* 7:585-599, 1951
12. Bárczai-Martos M, Kórösy F: Preparation of acetobrome-sugars. *Nature* 165:369, 1950
13. Chipowsky S, Lee YC: Synthesis of 1-thioaldosides having an amino group at the aglycon terminal. *Carbohyd Res* 31:339-346, 1973
14. Brown H: A study of 2,4,6-trinitrobenzesulfonic acid for automated amino acid chromatography. *Clin Chem* 14:967-978, 1968
15. Dubios M, Gilles KA, Hamilton JK, et al: Colorimetric method for determination of sugars and related substances. *Anal Chem* 28:350-356, 1956
16. Benjamin PP: A rapid and efficient method of preparing Tc-99m-human serum albumin: its clinical applications. *Int J Appl Radiat* 20:187-194, 1969
17. Dworkin HJ, Gutkowski RF: Rapid close-system production of Tc-99m-albumin using electrolysis. *J Nucl Med* 12:562-565, 1969
18. Jansholt AL, Krohn KA, Vera DR, et al: Radiochemical quality control using an inexpensive radiochromatogram scanner with analog and digital output. *J Nucl Med Technol* 8:222-227, 1980
19. Kozma C, Macklin W, Cummins LM, et al: Anatomy, physiology, and biochemistry of the rabbit. In *The Biology of the Laboratory Rabbit*, Weisbroth SH, Flatt RD, Kraus AL, eds. New York, Academic Press, 1974, pp 47-72
20. Horwitz DL, Ballantine TVN, Herman CM: Acute effects of septic shock on plasma and red cell volumes in baboons. *J Appl Physiol* 33:320-324, 1972
21. Snyder WS, Ford MR, Warner GG, et al: *'S' Absorbed Dose per Unit Cumulative Activity for Selected Radionuclides and Organs, MIRD Pamphlet No 11*. New York, Society of Nuclear Medicine, 1975
22. Bateman H: Solution of a system of differential equations occurring in the theory of radio-active transformations. *Proc Cambridge Phil Soc* 15:423-426, 1910
23. Bevington PR. *Data Reduction and Error Analysis for the Physical Sciences*, New York, McGraw Hill, 1969, pp 235-240
24. Vera DR, Krohn KA, Scheibe PO, et al: Identifiability analysis of an in vivo receptor-binding radiopharmacokinetic system. *IEEE Trans Biomed Eng* BME-32:312-322, 1985
25. Wagner JG: *Fundamentals of Clinical Pharmacokinetics*, Hamilton, IL, Drug Intelligence Publications, 1975, pp 22-24
26. MIRD Dose-Estimates Report No 3: Summary of current radiation dose estimates to humans with various liver conditions from Tc-99m sulfur colloid. *J Nucl Med* 16:108A, 1975